Structural properties of hyperbranched polymers in the melt under shear via nonequilibrium molecular dynamics simulation

Tu C. Le,[1] B. D. Todd,[1,a)] P. J. Daivis,[2] and A. Uhlherr[3]
[1]*Centre for Molecular Simulation, Swinburne University of Technology, P.O. Box 218, Hawthorn, Victoria 3122, Australia*
[2]*School of Applied Sciences, RMIT University, P.O. Box 2476V, Melbourne, Victoria 3001, Australia*
[3]*CSIRO Information Management and Technology, Private Bag 33, Clayton South, Victoria 3169, Australia*

(Received 30 October 2008; accepted 9 December 2008; published online 18 February 2009)

Hyperbranched polymer melts have been simulated using a coarse-grained model and nonequilibrium molecular dynamics (NEMD) techniques. In order to determine the shear-induced changes in the structural properties of hyperbranched polymers, various parameters were calculated at different strain rates. The radii of gyration which characterize the size of the polymer were evaluated. The tensor of gyration was analyzed and results indicate that hyperbranched polymer molecules have a prolate ellipsoid shape under shear. As hyperbranched polymers have compact, highly branched architecture and layers of beads have increasing densities which might lead to an unusual distribution of mass, the distribution of beads was also studied. The distribution of terminal beads was investigated to understand the spatial arrangement of these groups which is very important for hyperbranched polymer applications, especially in drug delivery. © *2009 American Institute of Physics*. [DOI: 10.1063/1.3077006]

I. INTRODUCTION

Hyperbranched polymers belong to a synthetic treelike macromolecule class called dendritic polymers which have received considerable interest over the past 20 years due to their unusual properties in comparison with linear polymers. They are polymers with densely branched structure and a large number of functional end groups. Dendritic polymers include dendrimers which have completely branched starlike topologies and hyperbranched polymers which are imperfectly branched or irregular structures, as shown in Fig. 1. For a given number of monomers with a specific branching architecture, there is only one dendrimer structure but a large number of hyperbranched structures can be formed because of different ways of distributing the branched and unbranched monomers.

The history of hyperbranched polymers can be traced back to the 19th century with the report of formation of a resin from tartaric acid and glycerol. It was not until 1978 that the first controlled synthesis of branched systems was reported by Buhleier *et al.*[1] and in 1988, the first hyperbranched polymer was finally synthesized in the form of soluble polyphenylene by Kim and Webster.[2,3] Since then, hyperbranched polymers have gained considerable attention from both academia and industry due to their unique properties and greater availability compared to dendrimers. One of the most interesting physical properties of hyperbranched polymers is their considerably different viscosity characteristics in comparison with linear analogs,[4,5] which can be explained by the architecture of the molecules. For linear polymers, the melt viscosity increases linearly up to a critical molar mass where the viscosity drastically increases as a consequence of the entanglement of polymer chains. However, this phenomenon is not observed for dendrimers or hyperbranched polymers which indicates that minimal entanglement of the branched chains occurs.[5,6] Other interesting properties of hyperbranched polymers are globular conformations and degree of branching. X-ray and small-angle neutron scattering experiments show that dendrimers have spherical conformations, while hyperbranched polymers have less symmetric, globular structures.[7] The degree of branching is reflected in the flexibility of the branching components contained within the architecture as well as the intrinsic viscosity of the polymer. Polymers with a higher degree of branching have lower intrinsic viscosity.

Due to their unique properties and easy synthesis, hyperbranched polymers have a wide range of potential applications. They have been used as rheology modifiers, blend components, or tougheners for thermosets as reported elsewhere.[5] In the early 1990s, it was found that adding a small amount of hyperbranched polyphenylenes to a polysty-

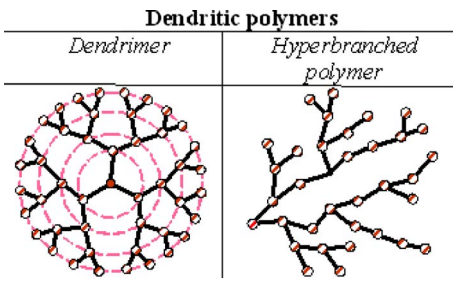

FIG. 1. (Color online) Comparison between trifunctional dendrimer and randomly branched hyperbranched polymer architectures (see Sec. II A for more details of the model actually simulated in this work).

a)Electronic mail: btodd@swin.edu.au.

rene melt greatly reduces the melt viscosity.[3] Because of the low cost and well-defined architecture with multifunctional terminal groups and narrow polydispersity, hyperbranched polymers have gained increasing attention in biomaterial applications.[5] Due to a large number of functional groups and interesting optical, electrochemical, biological, and mechanical properties of hyperbranched molecules, patterning of hyperbranched polymer films is also receiving increased attention.[5] Depending on the high solubility, low viscosity and abundant functional groups, hyperbranched polymers have been used as the base for various coating resins.[5] Hyperbranched polymers such as poly(phenylenevinylene) and polythiophenes have been used as conjugated functional materials because of their good solubility and excellent processibility.[5]

One of the first numerical studies of hyperbranched polymers was reported by Aerts[8] in 1998. Configurations of hyperbranched polymers were modeled using the bead model of Lescanec and Muthukumar[9] and intrinsic viscosities were calculated. It was shown that there is a maximum of intrinsic viscosity as a function of molecular weight but the maximum is situated at a higher level of intrinsic viscosity and shifted to higher molecular weights in comparison with dendrimers.[8] The limitations of this work are the application of the algorithm with no configurational relaxation and the questionable deduction of the intrinsic viscosity from the radius of gyration of branched structures.[10] Furthermore, this research employed the dense-shell model (density maximum at the periphery) which was first questioned by Boris and Rubinstein[11] who supported the validity of the dense-core one (density maximum at the center).

Also with the purpose of determining the intrinsic viscosities, a special class of hyperbranched polymers built by single stepwise addition of AB_2 monomer units to a B_3 core was modeled using a simple hydrocarbon model and the RIS Metropolis Monte Carlo procedure.[12] This model once again suggested that hyperbranched polymers should show a maximum in intrinsic viscosity at readily achievable branching ratios. Furthermore, it was found that the degree of branching is not an adequate descriptor for the shape of dendritic molecules and the Wiener index of the connectivity tree of a hyperbranched structure (defined as $W=(1/2)\Sigma_{j=1}^{N}\Sigma_{i=1}^{N}d_{ij}$ where N is the degree of polymerization and d_{ij} is the number of bonds separating bead i and j of the molecule) shows a near perfect power-law correlation with the simulated intrinsic viscosities of molecules with the same molecular weight but different topologies.[12] However, a phantom chain model without solvent was applied and this does not take into account excluded—volume effects which increase in highly crowded hyperbranched structures.[10]

In order to address some of the issues raised in these earlier papers, hyperbranched polymer solutions in simple shear flow were simulated by Lyulin *et al.*[10] using Brownian dynamics techniques. This method allows calculation of the intrinsic viscosity of a very dilute solution over a broad range of shear rates. Hydrodynamic and excluded-volume interactions were treated explicitly. Shear thinning effects were observed for all simulated degrees of branching and, similar to dendrimers, as the molecular weight increases, the zero shear rate intrinsic viscosity reaches a maximum and then begins to fall. On the other hand, a reduction or disappearance of the peak was observed when the degree of branching increased, which suggested that the degree of branching was an effective index to distinguish different intrinsic viscosity behaviors on a qualitative basis. Nevertheless, the degree of branching only accounts for the relative number of branch points and is insensitive to their distribution within the molecule.[13] Therefore, the Wiener index was used to characterize the different structures in further study.[13] Brownian dynamics simulation of hyperbranched polymers up to the sixth generation under elongational flow has also been reported,[14] in which the statistical and rheological properties of a bead-rod model of hyperbranched materials in solution were investigated.

Konkolewicz *et al.*[15] reported that the reverse Monte Carlo[16] technique was applied to generate randomly branched polymers with different architectures and sizes in solution. A logarithmic growth of radius of gyration with polymer mass was observed.

More recently Brownian dynamics has been applied[17] to simulate complexes formed by hyperbranched polymers with linear polyelectrolytes under steady shear flow. Static and dynamic properties of these complexes have been investigated. Konkolewicz *et al.*[18] also recently presented a comparison of Monte Carlo and molecular dynamics simulation with theoretical model conformation results including the radii of gyration and full density profiles for randomly hyperbranched polymers in solution.

Our aim in this paper is to extend the simulations on hyperbranched polymers further by conducting the first nonequilibrium molecular dynamics (NEMD) simulations of hyperbranched polymers in the melt and comparing our results with equivalent molecular weight linear polymers and dendrimers, as well as other published results. Systems away from equilibrium can be studied through the analysis of equilibrium correlation functions (i.e., via Green–Kubo relations) or by directly sampling a nonequilibrium ensemble. In this paper, the structural properties of dense hyperbranched polymer liquids under planar shear flow are analyzed. In a subsequent study, we will discuss the rheological properties of these fluids. The remainder of this paper is organized as follows. Section II describes the coarse-grained model used to simulate hyperbranched polymers and the NEMD algorithms applied. The definition of structural property parameters is also included. Section III presents the results and a discussion of the mean squared radii of gyration, eigenvalues of the tensor of gyration, distribution of mass and terminal groups, as well as the atomic radial distribution function. Some conclusions are presented in the final section.

II. METHODOLOGY

A. Hyperbranched polymer model

Hyperbranched polymers were simulated using coarse-grained[19] uniform beads. These basic units correspond to the linear units or branching points of the molecule and are interconnected to create treelike structures. Beads along the chain can rotate and vibrate freely. All beads are

identical and indistinguishable except for their position in the molecule. This coarse-grain bead model has been used in previous NEMD study for dendrimers.[20] The total number of beads in dendrimers can be defined as $N=fb((f-1)^{g+1}-1)/(f-2)+1$ where f is the functionality of end groups, b is the number of monomers in the chain units, and g is the generation number. With the choice of $f=3$ and $b=2$, dendrimers of generation 1, 2, 3, and 4 will have 19, 43, 91, and 187 beads, respectively. In order to compare our simulation data with those for dendrimers, the hyperbranched polymer chains generated in this work are composed of 19, 43, 91, and 187 interconnected beads. A simple specific architecture of hyperbranched polymers has been chosen. They are dendrimers with trifunctional end groups ($f=3$) and two beads in the chain units ($b=2$) that have one imperfect branching point ($f=2$). As hyperbranched polymers have the same number of beads as dendrimers but fewer branches at one branching point, extra beads are added in the outermost layer of the molecules with $f=3$ and $b=2$. Typical instantaneous configurations of simulated hyperbranched polymers are shown in Fig. 2.

In this model, only bond and pairwise interactions are taken into account, beads comprising the melt interact via Weeks–Chandler–Anderson[21] (WCA) and finitely extensible nonlinear elastic[22] (FENE) potentials. The WCA potential can be calculated as follows:

$$U_{ij}^{\mathrm{WCA}} = 4\varepsilon\left[\left(\frac{\sigma}{r_{ij}}\right)^{12} - \left(\frac{\sigma}{r_{ij}}\right)^{6}\right] + \varepsilon \quad \text{for } r_{ij}/\sigma < 2^{1/6},$$
$$U_{ij}^{\mathrm{WCA}} = 0 \quad \text{for } r_{ij}/\sigma \geq 2^{1/6}, \tag{1}$$

where r_{ij} is the separation between the sites represented by beads i and j, ε is the potential well depth, and σ is the effective diameter of the beads. This potential results in a purely repulsive force that includes the effect of excluded volume.

The FENE potential is given as

$$U_{ij}^{\mathrm{FENE}} = -0.5kR_0^2 \ln[1-(r_{ij}/R_0)^2] \quad \text{for } r_{ij} \leq R_0,$$
$$U_{ij}^{\mathrm{FENE}} = \infty \quad \text{for } r_{ij} \geq R_0, \tag{2}$$

where R_0 is a finite extensibility and k is a spring constant. In this work, these FENE parameters, R_0 and k, were set to 1.5 and 30, respectively. For this choice of parameters the maximal extent of bonds is short enough to prevent crossing of branches, whereas the magnitude of the bonding force is small enough to enable simulations with relatively large time steps.[20,23] The FENE chain model is not only suitable for entangled and unentangled polymer melts but is also applicable to monodisperse and polydisperse polymers.

Nonbonded beads only have WCA potential interactions whereas bonded beads have both FENE and WCA interactions which creates a potential well for the flexible bonds that maintains the architecture of the molecules.

In the remainder of this paper, all quantities are expressed in terms of site reduced units in which the reduction parameters are the Lennard-Jones interaction parameters ε and σ and the mass, $m_{i\alpha}$, of atom/bead α in molecule i. The reduced temperature is given by $T^*=k_BT/\varepsilon$, the density by $\rho^*=\rho\sigma^3$, the pressure tensor by $\mathbf{P}^*=\mathbf{P}\sigma^3/\varepsilon$ and strain rate by $\dot{\gamma}^*=(m\sigma^2/\varepsilon)^{1/2}\dot{\gamma}$. For simplicity of notation, the asterisk will be omitted hereafter.

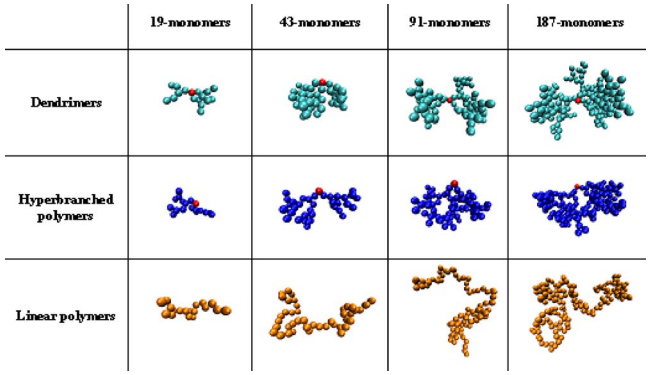

FIG. 2. (Color online) Configuration of simulated hyperbranched polymers in comparison with dendrimers and linear polymers.

B. NEMD simulation

To build a model of a hyperbranched polymer fluid, 216 molecules in the case of 19 bead polymers and 125 molecules for larger polymers were generated in a cubic simulation box which was surrounded by its periodic images. Lees–Edwards[24] shear boundary conditions were applied to eliminate effects associated with surfaces and the small volume of the system.

To simulate fluids under shear, the molecular version of the SLLOD algorithm[25] was applied. The reasons for using this version of the SLLOD algorithm have been discussed extensively elsewhere.[26] The equations of motion are given as

$$\dot{\mathbf{r}}_{i\alpha} = \frac{\mathbf{p}_{i\alpha}}{m_{i\alpha}} + \mathbf{r}_i \cdot \nabla\mathbf{u}, \tag{3}$$

$$\dot{\mathbf{p}}_{i\alpha} = \mathbf{F}_{i\alpha} - (m_{i\alpha}/M_i)\mathbf{p}_i \cdot \nabla\mathbf{u} - \zeta(m_{i\alpha}/M_i)\mathbf{p}_i, \tag{4}$$

where $\mathbf{r}_{i\alpha}$ and $\mathbf{p}_{i\alpha}$ represent the position and thermal momentum of an atom/bead α in molecule i, $\nabla\mathbf{u}$ is the velocity gradient tensor, $\mathbf{r}_i=\Sigma_{\alpha=1}^{N_\alpha} m_{i\alpha}\mathbf{r}_{i\alpha}/M_i$ is the position of the molecular center of mass of molecule i, $M_i=\Sigma_{\alpha=1}^{N_\alpha} m_{i\alpha}$ is the mass of molecule i, $\mathbf{p}_i=\Sigma_{\alpha=1}^{N_\alpha}\mathbf{p}_{i\alpha}$ is the momentum of the molecular center of mass of molecule i and ζ is the thermostat constraint multiplier which is given by Eq. (5). All simulations were performed at constant volume at a reduced temperature[27] of 1.25. To keep the translational kinetic temperature fixed, the molecular version of the Gaussian isokinetic thermostat has been used. ζ is determined by the condition that the molecular kinetic energy is constant and the deviations of the trajectories from the unthermostated ones is minimized.

$$\zeta = \frac{\Sigma_{i=1}^{N}\mathbf{F}_i \cdot \mathbf{p}_i - \dot{\gamma}\Sigma_{i=1}^{N} p_{ix}p_{iy}}{\Sigma_{i=1}^{N}\mathbf{p}_i^2}. \tag{5}$$

To prepare the initial configuration for the simulation of the melts under shear, only diagonal elements of the velocity gradient tensor are nonzero:

$$\nabla \mathbf{u} = \begin{pmatrix} \dot{\varepsilon}_{xx} & 0 & 0 \\ 0 & \dot{\varepsilon}_{yy} & 0 \\ 0 & 0 & \dot{\varepsilon}_{zz} \end{pmatrix}. \tag{6}$$

If all these elements are positive, the equations of motion will correspond to expansion at a steady rate. If these values are negative, the equations of motion will correspond to compression. In this work, the system of molecules was generated at a low density and then compressed until the required bead number density (ρ=0.84) was achieved. When only one off-diagonal element of the velocity gradient tensor is nonzero

$$\nabla \mathbf{u} = \begin{pmatrix} 0 & 0 & 0 \\ \dot{\gamma}_{yx} & 0 & 0 \\ 0 & 0 & 0 \end{pmatrix}, \tag{7}$$

the algorithm corresponds to planar Couette flow.

The equations of motion of atoms were integrated with time step Δt=0.001 in reduced units using a fifth-order Gear predictor corrector differential equation solver.[28]

C. Structural analysis

The mean square radius of gyration tensor of molecules can be calculated according to the formula:

$$\mathbf{R}_g^2 \equiv \left\langle \frac{\Sigma_{\alpha=1}^{n} m_\alpha (\mathbf{r}_\alpha - \mathbf{r}_{\mathrm{CM}})(\mathbf{r}_\alpha - \mathbf{r}_{\mathrm{CM}})}{\Sigma_{\alpha=1}^{n} m_\alpha} \right\rangle, \tag{8}$$

where $\mathbf{r}_a$ is the position of bead α, $\mathbf{r}_{\mathrm{CM}}$ is the position of the molecular center of mass and the angle brackets denote an ensemble average. The value of the squared radius of gyration which is defined as the trace of the tensor ($R_g^2 = \mathrm{Tr}(\mathbf{R}_g^2)$) characterizes the size of the molecule.

By studying the tensor of gyration, the shape of hyperbranched polymers can be investigated. The ensemble averaged eigenvalues (L_1, L_2, and L_3) of the tensor of gyration were calculated to analyze flow-induced changes in the shape of the molecules as the flow-induced stretching of hyperbranched polymers together with molecular alignment can lead to the macroscopic anisotropy of the material.[20] In order to calculate these ensemble averaged eigenvalues, the tensor of gyration was diagonalized separately for each molecule in the system. Using this approach, the shape of the hyperbranched polymer molecule can be studied disregarding the molecular orientation. The ratios of these eigenvalues, which describe the asymmetry of hyperbranched polymers, were also calculated. The results for the ensemble averaged tensor of gyration prior to its diagonalization have also been computed and eigenvalues (L_1', L_2', and L_3') were analyzed. In this approach, all elements of the tensor of gyration are averaged over all molecules and time separately, the shape of a mean molecule is obtained from superposition of all molecules in the system and these eigenvalues can be considered as the linear dimensions of the ellipsoid occupied by the molecule in the laboratory frame of Ref. 29.

Hyperbranched polymers have a compact, globular structure due to their densely branched architecture. This might lead to an unusual distribution of mass. To analyze the distribution of mass within the molecule, two forms of intramolecular radial distribution function have been used. The first function, which measures the distribution of beads from the central bead (the core), is defined as

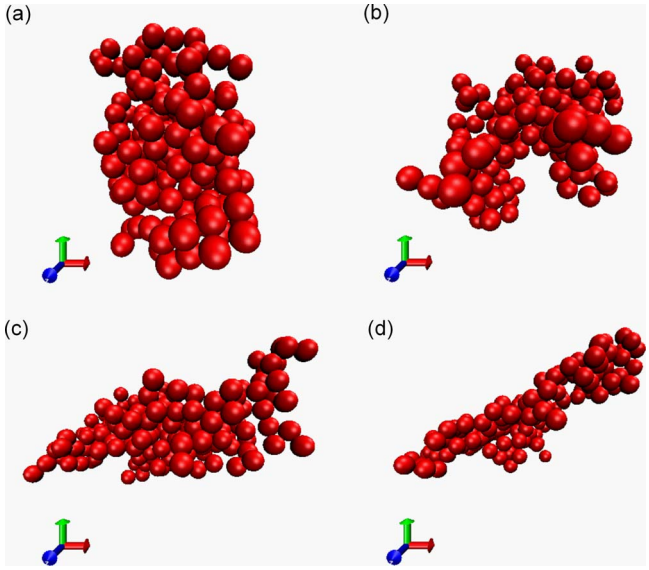

FIG. 3. (Color online) Configuration of hyperbranched polymers with 187 monomers at strain rates of (a) 0.0001, (b) 0.001, (c) 0.01, and (d) 0.1.

$$g_{\mathrm{core}}(r) = \frac{\langle \Sigma_{i=1}^{N} \Sigma_{\alpha=2}^{N_s} \delta(|\mathbf{r} - (\mathbf{r}_{i\alpha} - \mathbf{r}_{i1})|) \rangle}{N}, \tag{9}$$

where $\mathbf{r}_{i1}$ is the position of the core, N_s is the number of sites/beads per molecule, and α runs over all other beads belonging to the same molecule. The second function, which measures the distribution of beads from the molecular center of mass, is defined as

$$g_{\mathrm{CM}}(r) = \frac{\langle \Sigma_{i=1}^{N} \Sigma_{\alpha=1}^{N_s} \delta(|\mathbf{r} - (\mathbf{r}_{i\alpha} - \mathbf{r}_{\mathrm{CM}})|) \rangle}{N}, \tag{10}$$

where $\mathbf{r}_{CM}$ is the position of the center of mass.

The radial distribution function of the terminal groups with reference to the central bead was also investigated to analyze the entanglement and back folding in the molecules:

$$g_{\mathrm{term}}(r) = \frac{\langle \Sigma_{i=1}^{N} \Sigma_{\alpha=1}^{N_s} \delta(|\mathbf{r} - (\mathbf{r}_{i\alpha} - \mathbf{r}_{i1})|) \rangle}{4\pi r^2 N}, \tag{11}$$

where this time α runs over the outermost beads only.

The atomic radial distribution function which is defined by

$$g_A(r) = \frac{\left\langle \frac{1}{2} \Sigma_{i=1}^{N_{\mathrm{total}}} \Sigma_{j \neq i}^{N_{\mathrm{total}}} \delta(|\mathbf{r} - \mathbf{r}_{ij}|) \right\rangle}{4\pi r^2 N_{\mathrm{total}} \rho}, \tag{12}$$

where $\mathbf{r}_{ij}$ is the distance between the beads i and j, $N_{\mathrm{total}} = NN_s$ is the total number of beads in the studied system, and ρ is the density, is extensively used to study the internal structure and spatial ordering of atoms comprising materials. The function $g_A(r)$ gives the probability of finding two beads at the separation r.

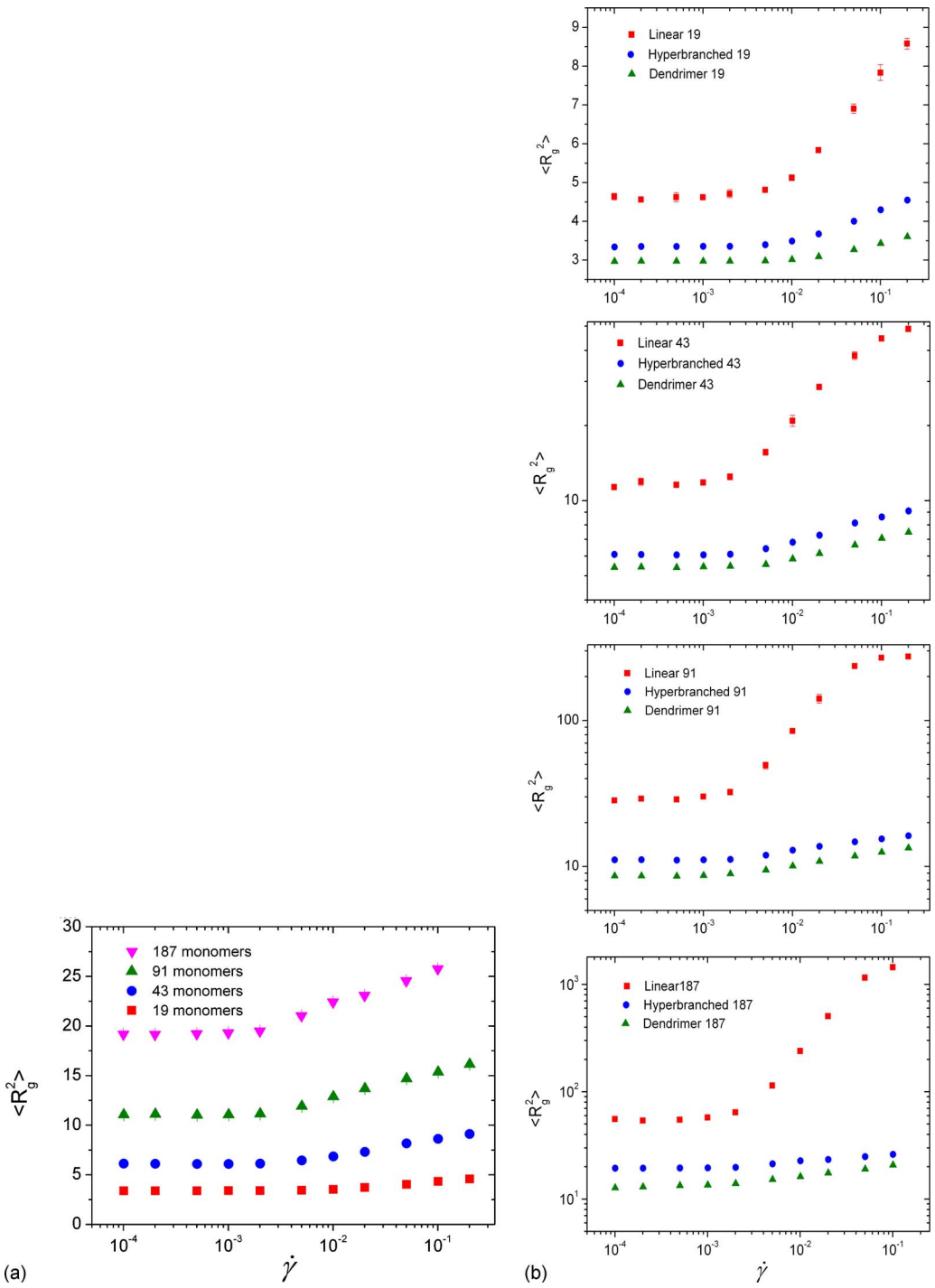

FIG. 4. (Color online) (a) Mean squared radii of gyration of polymers at different strain rates. (b) Comparison of radii of gyration for hyperbranched polymers, dendrimers, and linear polymers.

III. RESULTS AND DISCUSSION

In contrast to previous studies which addressed the simulation of hyperbranched polymers in solution, this work focuses on the properties of these macromolecules in the melt away from equilibrium. Structural properties of hyperbranched polymers in the melt under shear have been analyzed. Figure 3 illustrates the changes in shape and orientation of hyperbranched polymers with 187 monomers over a wide range of strain rates. It can be seen that at high strain rates, hyperbranched polymer molecules are more stretched, as is to be expected.

Radii of gyration, which indicate the extension of a molecule, are shown in Fig. 4. The analysis of the radius of gyration gives information about the mean spatial distribution inside the molecules regardless of their shapes. These simulated values are often compared to experimental results using light scattering, small-angle neutron scattering, and small-angle x-ray scattering methods which are well established in polymer science. As at this stage we only look at idealized hyperbranched polymer architecture with one specific imperfect point, radius of gyration results cannot be compared directly to experimental data for randomly

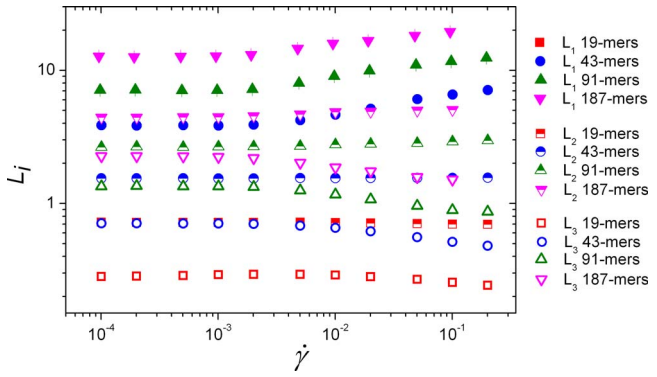

FIG. 5. (Color online) Averaged eigenvalues of the tensor of gyration for different hyperbranched polymers.

branched polydisperse systems. In future work, we hope to study more complex architectures that should allow comparison with scattering results. Figure 4(a) presents the dependence of the radii of gyration for different hyperbranched polymers on strain rate. For all studied systems, at small strain rates, the size of the polymer remains constant but for large values of strain rate, the values of $\langle R_g^2 \rangle$ increase, indicating that molecules are stretched under shear. For a given value of strain rate, the extent of shear-induced stretching increases with the number of beads. As shown in Fig. 4(b), in comparison with results from previous simulations,[20] the radii of gyration for hyperbranched polymers are in the range between those of dendrimers and linear polymers of equivalent molecular weight. This can be explained by the architecture of the molecules. With the same number of monomers, dendrimer structures on average have the most compact geometry with the smallest spatial separation of monomers, whereas hyperbranched polymers are less compact, while linear polymers have the largest distances between monomers.

The tensor of gyration is a useful parameter to characterize the structural properties and alignment of the molecules. The mean shape of a polymer molecule in the system is characterized by the ensemble averaged eigenvalues L_1, L_2, and L_3 of the tensor of gyration which was diagonalized separately for each molecule. As shown in Fig. 5, for all systems simulated, the values of L_1 are always much higher than L_2 and L_3 which are very similar. This indicates that hyperbranched polymers have a prolate ellipsoidal shape. In comparison with other NEMD simulation results,[20] the eigenvalues of the tensor of gyration for hyperbranched polymers are in the range between those of linear polymers and dendrimers but slightly higher than the eigenvalues for dendrimers. This shows that the prolate ellipsoidal shape of hyperbranched polymer molecules is very similar to dendrimers but somewhat flatter. The variation of these values is related to the stretching of the molecules and becomes significant at high strain rates. The comparison of average eigenvalues of the tensor of gyration for polymers with different chain lengths is also presented. These values show very similar trends.

The asymmetry of hyperbranched polymers is characterized by the ratio of the eigenvalues of the average gyration tensor. If the ratios of the eigenvalues are closer to 1, the

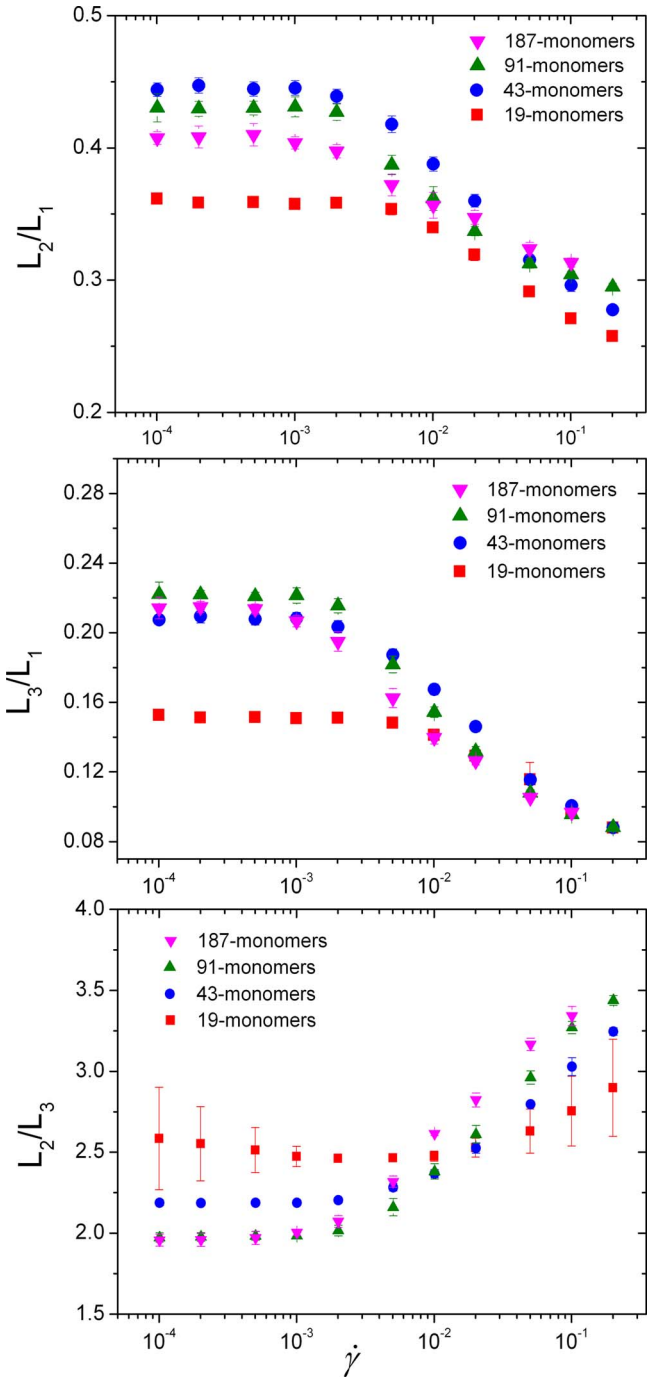

FIG. 6. (Color online) Ratios of averaged eigenvalues of the tensor of gyration for different hyperbranched polymers.

molecules have greater spherical symmetry. Like dendrimers and linear polymers, hyperbranched polymer molecules are stretched under shear. The differences between the eigenvalues of the tensor of gyration increase with the increase in strain rate and there is a noticeable change in the slopes of these ratios at similar strain rates as can be seen in Fig. 6. Previous investigations have shown that for dendrimers, with increasing number of beads, the molecules become more spherical, whereas for linear polymers, an opposite trend is observed.[29] It is interesting that smaller molecules of hyperbranched polymers become aspherical under shear more slowly than larger molecules of hyperbranched polymers. In

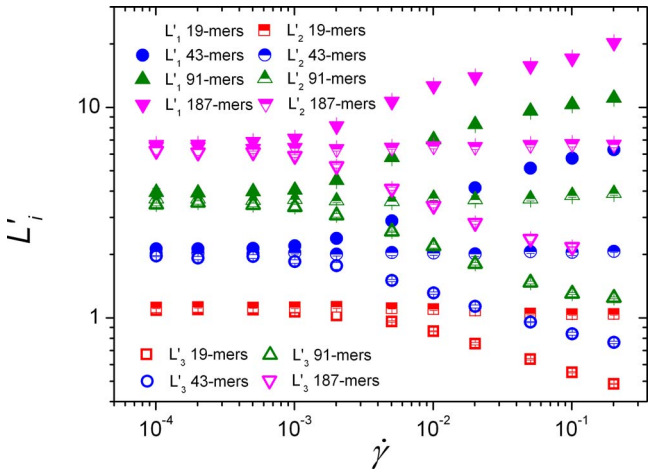

FIG. 7. (Color online) Eigenvalues of the average tensor of gyration for different hyperbranched polymers in comparison with dendrimers and linear polymers of equivalent molecular weight.

other words, small hyperbranched chains tend to retain their cross section when stretched, while larger chains extend by contracting in their smallest dimension (i.e., they become flatter).

The eigenvalues of the average tensor of gyration for hyperbranched polymers, which was calculated prior to diagonalization, also reflect the degree of orientation of the molecules. They can be interpreted as the linear dimensions of the prolate ellipsoid occupied by the orientationally averaged molecule. For hyperbranched polymers, the eigenvalues of the average tensor of gyration are equal at equilibrium because of orientational disorder and depart from this equilibrium value right from the smallest strain rates, as shown in Fig. 7. This demonstrates the onset of flow-induced molecular deformation. It can also be seen from Fig. 7 that the eigenvalues of the average tensor of gyration for hyperbranched polymers of different sizes have very similar trends due to their similar behavior under shear flow.

Ratios of the eigenvalues of the average tensor of gyration can be found in Fig. 8. The ratio between L_2' and L_1' as well as that between L_3' and L_1' decrease with increasing strain rates. An opposite trend was observed for the ratio between L_2' and L_3' which increase with increasing strain rates. These behaviors are caused by the fact that hyperbranched polymers become more stretched along the flow axis and lead to the faster growth of L_1' with strain rates compared to the increase of L_2' and L_3'. These ratio values for hyperbranched polymers are again in the range between those for linear polymers and dendrimers due to their molecular topologies. Unlike the case of the average eigenvalues of the tensor of gyration, the eigenvalues of the average tensor of gyration show very similar trends for dendrimers, linear and hyperbranched polymers.

The distribution of mass from the central unit (core) for different hyperbranched polymer systems at the strain rate of 0.0001 and 0.1 can be found in Fig. 9, whereas the distribution of mass from the center of mass at those strain rates is shown in Fig. 10. In all cases, the distributions of mass for polymers with different chain lengths always show a similar trend. The correlation between the position of the core and

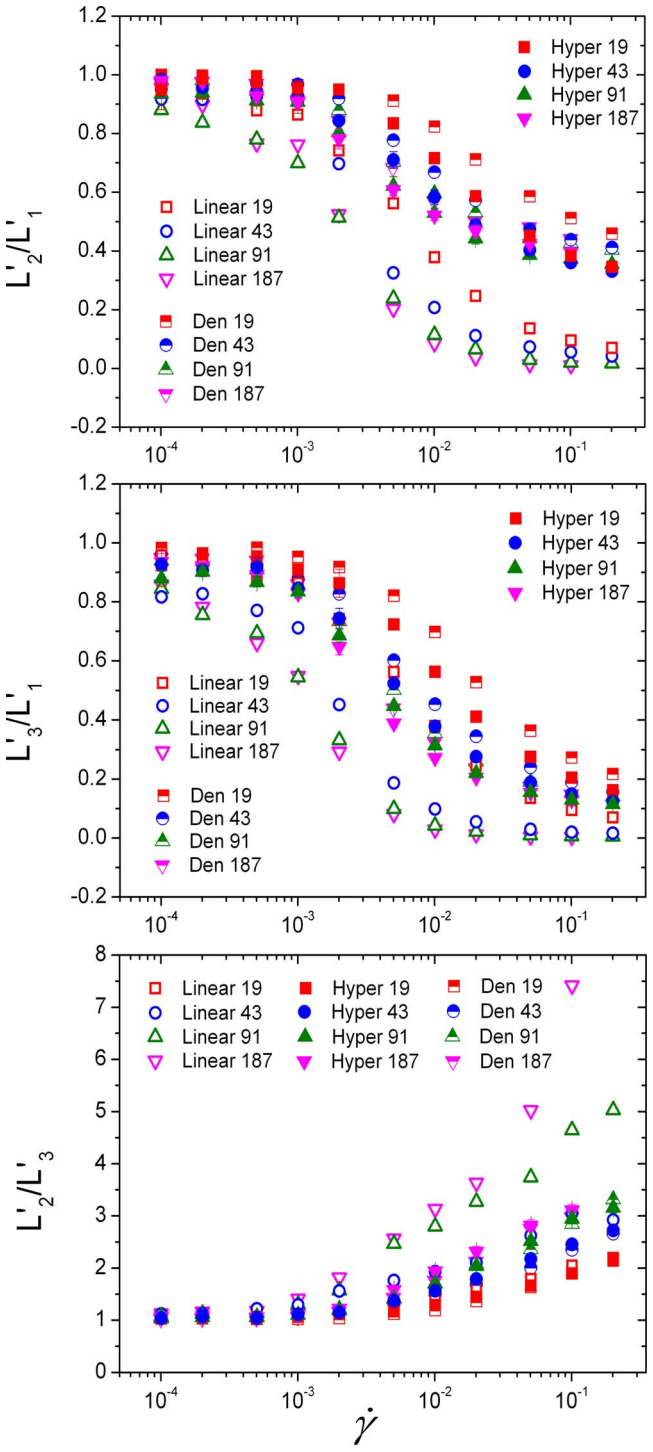

FIG. 8. (Color online) Ratios of eigenvalues of the average tensor of gyration for different hyperbranched polymers in comparison with those of dendrimers and linear polymers.

its first neighbors is evident through a strong peak at the distance equal to the average bond length. At high strain rates, as the molecules are stretched in the flow, the distribution of mass becomes broader and the average distance of beads from the center of mass increases with the strain rate. For the largest strain rates considered, the maximum distance between beads and the center of mass is comparable to the lengths of fully stretched arms of the polymers. The radial

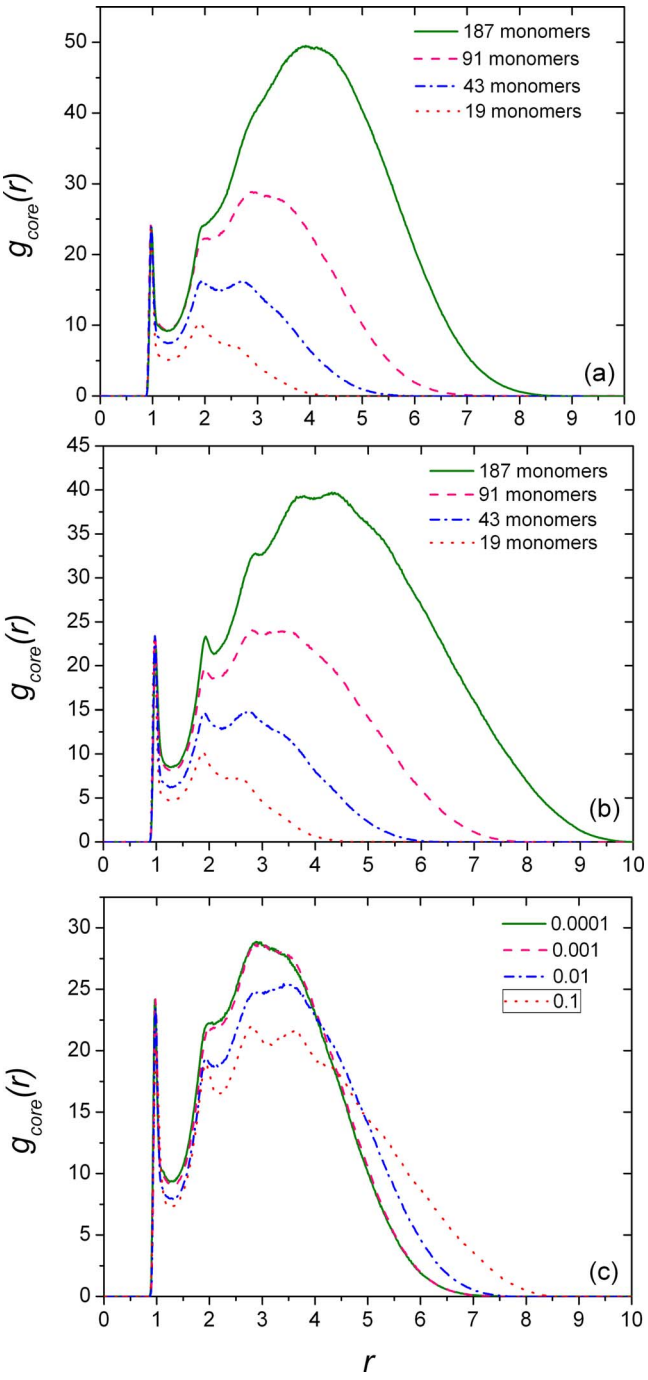

FIG. 9. (Color online) Distribution of beads from the core for different hyperbranched polymers at strain rates of (a) 0.0001, (b) 0.1, and (c) for hyperbranched polymers with 91 monomers at various strain rates.

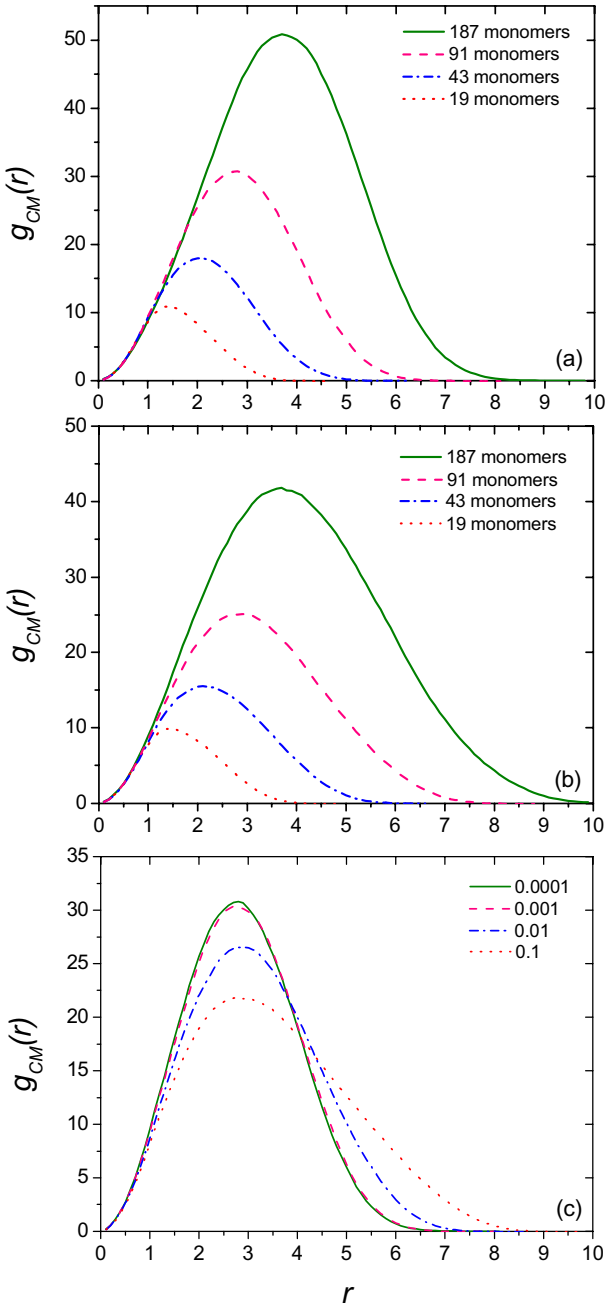

FIG. 10. (Color online) Distribution of beads from the center of mass for different hyperbranched polymers at strain rates of (a) 0.0001, (b) 0.1, and (c) for hyperbranched polymers with 91 monomers at various strain rates.

distribution of bead position relative to the center of mass has also been computed for different architectures of hyperbranched polymers comprising 190 beads using the Brownian dynamics technique.[14] The distribution function for hyperbranched polymers in solution only shows the first peaks that correspond to near neighbors and then decreases steadily as the distance from the core increases. It was also found that the decay in these functions is slower for hyperbranched polymers with lower degree of branching values because these structures are less compact. Furthermore, increasing strain rate leads to a more regular distribution of chain monomers along the flow axis and the extent of this regularity is not as pronounced for trifunctional polymers as for bifunctional systems.

One of the characteristic properties of hyperbranched polymers is the large number of terminal groups, from which hyperbranched polymers are characterized as active molecules with high solubilities and this leads to a number of applications, especially in drug delivery. In Fig. 11, we present the distribution of terminal groups from the central unit at the strain rate of 0.0001 when the system is close to equilibrium and at a high strain rate of 0.1. In all cases, secondary maxima are observed in the plot of distribution of terminal groups. This indicates that not all of the end groups

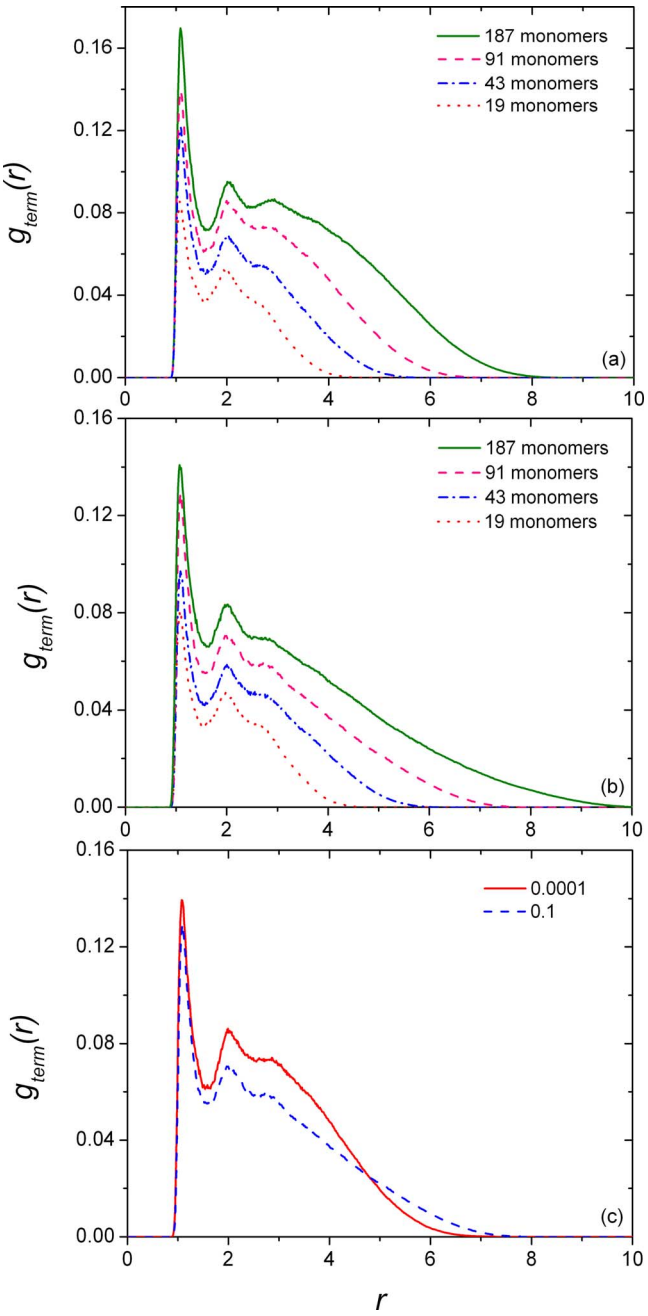

FIG. 11. (Color online) Distribution of terminal groups for different hyperbranched polymers at strain rates of (a) 0.0001, (b) 0.1, and (c) hyperbranched polymers with 91 monomers at different strain rates

are located on the surface of the molecules, but rather that they can be found across the full range of distances from the center unit due to backfolding. This means that terminal groups exist everywhere throughout the interior of the molecules. Other experimental[30] and simulation[9,20,30,31] results have also shown similar backfolding behaviors of dendrimers with peaks observed in the plot of distribution of end groups. Furthermore, Hsieh *et al.*[32] who reported experimental results for the melt rheology of commercial aliphatic hyperbranched polyesters, also found that hyperbranched polymers with larger molecular weight showed more inward chain folding of the terminal hydroxyl groups than polymers with smaller molecular weight. This effect, along with the lower or higher concentration of hydroxyl end groups per mass of polymers, led to weaker or stronger interactions affecting the Newtonian and non-Newtonian behaviors that were observed.

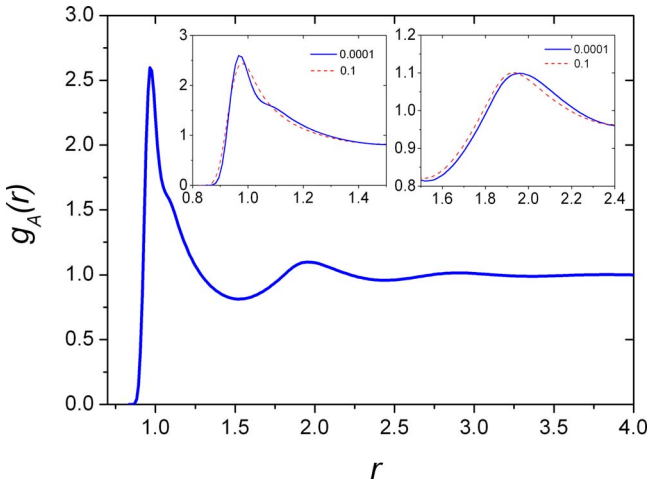

FIG. 12. (Color online) Atomic radial distribution function for hyperbranched polymer with 91 monomers at strain rates of 0.0001 and 0.1.

Atomic radial distribution results are shown in Fig. 12. In all cases, only the few first peaks which correspond to the shells of near neighbors can be observed. No significant changes could be distinguished in the atomic radial distribution functions of hyperbranched polymers with their size, as the distributions of different hyperbranched polymers virtually overlap. It can also be seen that the shear causes only small changes in the distribution function: the first peak becomes wider whereas the second peak is shifted toward smaller distances. For the present potential model, the first and strongest peak of the atomic radial distribution is contributed from two types of first neighbors. The first type includes beads that are chemically bonded to the central one and interact via both WCA and FENE potentials whereas the second type refers to all other beads that are close to the core and interact via only the WCA potential.

IV. CONCLUSIONS

The shearing behavior of hyperbranched polymers in the melt has been reported by NEMD simulations. Most of the microscopic structural properties have significant changes induced by the shear flow, which depend on the size and geometry of the molecules. Radius of gyration results indicates that molecules are stretched under shear and larger molecules have more flow-induced changes than the smaller ones. Analysis of the tensor of gyration shows that hyperbranched polymer molecules have a prolate ellipsoid shape which is slightly flatter than the ellipsoid shape of dendrimers. The conformational behavior of large hyperbranched polymers is similar to that of linear polymers whereas for small hyperbranched polymers, the behavior is similar to that of dendrimers. Having similar structures to dendrimers, simulated hyperbranched polymers show similar distribution of mass with terminal groups existing everywhere inside the molecules.

Rheological properties of these hyperbranched polymers and results for different architectures of hyperbranched polymers with the same molecular size will be reported in future work. The motivation and also one of our final goals is to successfully simulate polydisperse blends of linear and hyperbranched polymers for application as rheology modifiers. Another valuable extension would be the simulation of dendronized polymer systems which have the highest level of structural complexity presently known for synthetic polymers with applications spanning from single molecule chemistry to surface patterning.[33]

ACKNOWLEDGMENTS

We would like to thank Swinburne University of Technology Supercomputer Facility for a generous grant of computer time. One of the authors (T.C.L.) would like to thank Dr. Jaroslaw Bosko for his valuable suggestions and discussions.

[1] E. Buhleier, W. Wehner, and F. Vögtle, Synthesis **2**, 155 (1978).
[2] Y. H. Kim and O. W. Webster, Macromolecules **25**, 5561 (1992); Y. H. Kim and O. W. Webster, Polymer Preparation **23**, 310 (1988).
[3] Y. H. Kim and O. W. Webster, J. Am. Chem. Soc. **112**, 4592 (1990).
[4] C. R. Yates and W. Hayes, Eur. Polym. J. **40**, 1257 (2004); M. Jikei and M. Kakimoto, Prog. Polym. Sci. **26**, 1233 (2001).
[5] C. Gao and D. Yan, Prog. Polym. Sci. **29**, 183 (2004).
[6] E. Malmstrom and A. Hult, J. Macromol. Sci., Rev. Macromol. Chem. Phys. **C37**, 555 (1997); J. T. Bosko, B. D. Todd, and R. J. Sadus, J. Chem. Phys. **121**, 12050 (2004).
[7] T. J. Prosa, B. J. Bauer, E. J. Amis, D. A. Tomalia, and R. Scherrenberg, J. Polym. Sci., Part B: Polym. Phys. **35**, 2913 (1997).
[8] J. Aerts, Comput. Theor. Polym. Sci. **8**, 49 (1998).
[9] R. L. Lescanec and M. Muthukumar, Macromolecules **23**, 2280 (1990).
[10] A. V. Lyulin, D. B. Adolf, and G. R. Davies, Macromolecules **34**, 3783 (2001).
[11] D. Boris and M. Rubinstein, Macromolecules **29**, 7251 (1996).
[12] A. H. Widmann and G. R. Davies, Comput. Theor. Polym. Sci. **8**, 191 (1998).
[13] P. F. Sheridan, D. B. Adolf, A. V. Lyulin, I. Neelov, and G. R. Davies, J. Chem. Phys. **117**, 7802 (2002).
[14] I. M. Neelov and D. B. Adolf, J. Phys. Chem. B **108**, 7627 (2004).
[15] D. Konkolewicz, G. R. Gilbert, and A. Gray-Weale, Phys. Rev. Lett. **98**, 238301 (2007).
[16] C. J. C. Watts, A. Gray-Weale, and R. G. Gilbert, Biomacromolecules **8**, 455 (2007).
[17] G. K. Dalakoglou, K. Karatasos, S. V. Lyulin, and A. V. Lyulin, J. Chem. Phys. **129**, 034901 (2008).
[18] D. Konkolewicz, O. Thorn-Seshold, and A. Gray-Weale, J. Chem. Phys. **129**, 054901 (2008).
[19] C. N. Likos, Soft Matter **2**, 478 (2006).
[20] J. T. Bosko, B. D. Todd, and R. J. Sadus, J. Chem. Phys. **121**, 1091 (2004).
[21] J. D. Weeks, D. Chandler, and H. C. Anderson, J. Chem. Phys. **54**, 5237 (1971).
[22] G. S. Grest and K. Kremer, Phys. Rev. A **33**, 3628 (1986).
[23] M. Kroger, W. Loose, and S. Hess, J. Rheol. **37**, 1057 (1993).
[24] A. W. Lees and S. F. Edwards, J. Phys. C **5**, 1921 (1972).
[25] D. J. Evans and G. P. Morriss, *Statistical Mechanics of Nonequilibrium Liquids* (Academic, London, 1990).
[26] B. D. Todd and P. J. Daivis, Mol. Simul. **33**, 189 (2007).
[27] R. J. Sadus, *Molecular Simulation of Fluids: Algorithms and Object-Orientation* (Elsevier, Amsterdam, 1999).
[28] C. W. Gear, *Numerical Initial Value Problems in Ordinary Differential Equations* (Prentice-Hall, Englewood Cliffs, 1971).
[29] J. T. Bosko, B. D. Todd, and R. J. Sadus, J. Chem. Phys. **124**, 044910 (2006).
[30] I. Bodnar, A. S. Silva, R. W. Deitcher, N. E. Weisman, Y. H. Kim, and N. J. Wagner, J. Polym. Sci., Part B: Polym. Phys. **38**, 857 (2000).
[31] E. G. Timoshenko, Y. A. Kuznetsov, and R. Connolly, J. Chem. Phys. **117**, 9050 (2002).
[32] T. T. Hsieh, C. Tiu, and G. P. Simon, Polymer **42**, 1931 (2001); T. T. Hsieh, C. Tiu, and G. P. Simon, *ibid.* **42**, 7635 (2001).
[33] Y. Ding, H. C. Ottinger, A. D. Schluter, and M. Kroger, J. Chem. Phys. **127**, 094904 (2007); M. Kroger, O. Peleg, Y. Ding, and Y. Rabin, Soft Matter **4**, 18 (2008).